BIOCHEMICAL PHARMACOLOGY 72 (2006) 541–550

available at www.sciencedirect.com

ScienceDirect

journal homepage: www.elsevier.com/locate/biochempharm

8-Chloro-adenosine inhibits growth at least partly by interfering with actin polymerization in cultured human lung cancer cells

Yan-Yan Gu [a], Hong-Yu Zhang [a], Hai-Jun Zhang [a], Shu-Yan Li [a], Ju-Hua Ni [a], Hong-Ti Jia [a,b,*]

[a] Department of Biochemistry and Molecular Biology, Peking University Health Science Center, Xue Yuan Road 38, Beijing 100083, PR China

[b] Department of Biochemistry and Molecular Biology, Capital University of Medical Sciences, You An Men Xitoutiao 8, Beijing 100054, PR China

ARTICLE INFO

Article history:
Received 29 March 2006
Accepted 16 May 2006

Keywords:
8-Chloro-adenosine
G/F-actin ratio
Actin polymerization
G2/M arrest
Human lung cancer cell

ABSTRACT

A key feature of actin is its ability to bind and hydrolyze ATP. 8-Chloro-adenosine (8-Cl-Ado), which can be phosphorylated to the moiety of 8-Cl-ATP in living cells, inhibits tumor cell proliferation. Therefore we tested the hypothesis that 8-Cl-Ado can interfere with the dynamic state of actin polymerization. We found that 8-Cl-Ado inhibited the growth of human lung cancer cell line A549 and H1299 in culture, and arrested the target cells in G2/M phase evidenced by fluorescence-activated cell sorting (FACS). Immunocytochemistry showed that the normal organization of microfilaments was disrupted in 8-Cl-Ado-exposed cells, which is accompanied by the decrease of cell size and the alteration of cell shape, and by aberrant mitosis and apoptosis in targeted cells. Furthermore, *in vitro* light scattering assays revealed that 8-Cl-ATP could directly inhibit the transition of G-actin to F-actin. DNase I inhibition assays showed that the G/F-actin ratio, a surrogate marker of actin polymerization status in living cells, was significantly increased in 8-Cl-Ado-exposed A549 and H1299 cells, compared to the G/F-actin ratio in unexposed cells. Taken together, these results indicate that 8-Cl-Ado exposure can alter the dynamic properties of actin polymerization, disrupt the dynamic instability or the rearrangement ability of actin filaments. Therefore, our data suggest that 8-Cl-Ado may exert its cytotoxicity at least partly by interfering with the dynamic instability of microfilaments, which may correlate with its inhibitory effects on cell proliferation and cell death.

© 2006 Elsevier Inc. All rights reserved.

1. Introduction

Actin is the most abundant protein in a eukaryotic cell and organized into bundles and networks of filaments. Actin exists as a globular monomer called G-actin and as a filamentous polymer called F-actin, which is a linear chain of G-actin subunits. The ability of actin to polymerize into filaments and to depolymerize permits the rapid rearrangements of actin structures that are essential for actin's function in most cellular processes including cell growth and division, motility,

* *Corresponding author at.* Department of Biochemistry and Molecular Biology, Peking University Health Science Center, Xue Yuan Road 38, Beijing 100083, PR China. Tel.: +86 10 82801434; fax: +86 10 82801434.
E-mail address: jiahongti@bjmu.edu.cn (H.-T. Jia).

0006-2952/$ – see front matter © 2006 Elsevier Inc. All rights reserved.
doi:10.1016/j.bcp.2006.05.026

signaling, and the development and maintenance of cell shape [1]. Filament and dynamic property is conferred by the hydrolysis of ATP to ADP and P_i. Release of inorganic phosphate (P_i) from filaments after ATP hydrolysis permits depolymerization. The interconversion between the ATP and ADP forms of actin is crucial to the cellular functions of the cytoskeletal proteins [1,2].

Actin disruption prevents nuclear division, which is explained as activation of a morphogenesis checkpoint monitoring the integrity of the actin cytoskeleton [3]. The analysis of the kinetics of mitotic initiation after actin disruption in undersized and oversized cells shows that cells with a completely depolymerized actin cytoskeleton arrest in G2/M phase, due to an inability to reach the mitotic size threshold, suggesting that G2/M arrest caused by actin disruption is a manifestation of the cell size checkpoint [4].

The cytoskeletal proteins including actin and tubulin are the targets of a growing number of anti-cancer drugs [2]. Recent studies have indicated that alterations in the dynamic state of actin can change cell fate or induce cell death, which may be caused by actin-binding drugs [2,5,6], and by the mutations of actin or actin-binding proteins [7].

8-Chloro-cyclic-adenosine monophosphate (8-Cl-cAMP) is a potential anti-cancer drug [8–19]. Recent studies demonstrate that 8-Cl-cAMP exerts its cytotoxicity by converting into its metabolite, 8-chloro-adenosine (8-Cl-Ado) [9,17,18,20,21]. In living cells 8-Cl-Ado can be phosphorylated to the moiety of 8-Cl-ATP that inhibits the tumor cell proliferation through inhibition of RNA synthesis [17,18,22,23]. We have previously reported that 8-Cl-Ado can induce G2/M arrest in human lung cancer cell line A549 and H1299, followed by mitotic catastrophe [24]. In those studies, however, we have not clarified the mechanism of 8-Cl-Ado action on G2/M arrest coupled with actin organization. Because the transition from ATP-bound actin to ADP-bound actin is accompanied by a conformational change that is crucial to the dynamic turnover of actin filaments, we tested the hypothesis that 8-Cl-Ado may interfere with the dynamic state of actin. We found that 8-Cl-Ado could inhibit the polymerization of G-actin into F-actin filaments and disrupt actin filament organization in cultured lung cancer cells, which may correlate with 8-Cl-Ado-induced G2/M arrest and cell death and mitotic dividing failure. Our results suggest that 8-Cl-Ado may exert its cytotoxicity at least partly by interfering with the dynamic instability of microfilaments.

2. Materials and methods

2.1. Cell culture and chemical treatment

Human lung cancer cell lines A549 (p53-wt) and H1299 (p53-depleted) were purchased from the American Type Cell Culture (ATCC; Rockvill, MD). The cells were cultured in RPMI Medium 1640 (Life Technologies, Inc., Grand Island, NY, USA) supplemented with 10% fetal bovine serum (GIBCO BRL), 100 U/ml of penicillin, and 100 μg/ml streptomycin, and grown in a 37 °C incubator with 5% CO_2.

Twenty-four hours prior to experiments, 1.5×10^6 cells were plated on 75 cm^2 plates for DNase I assay of G-actin and total actin, and 5×10^4 cells were plated on the round coverslips $d = 1$ cm, which were placed in each well of 24-well dishes for immunocytochemical labeling. 8-chloro-adenosine (8-Cl-Ado) (the State Laboratory for Natural and Biomimetic Drugs, Peking University HSC, Beijing, China) was dissolved in sterilized 0.85% NaCl solution, and added to cultures at the concentration of 2 μM for 24, 48, 72 and 96 h, respectively. For control experiments, 0.85% NaCl solution was used. Cytochalasin B (CB) (C6762, Sigma–Aldrich Co.) was dissolved in DMSO, and added to cultures at the concentration of 2 μg/ml, DMSO as control.

2.2. Cell proliferation assay (MTT method)

This assay was performed as described previously [24]. Twenty-four hours prior to the experiment, the cells were cultured into 96-well dishes (15,000 cells/0.2 ml per well). 8-Cl-Ado of 0, 0.02, 0.2, 2, and 20 μM was added to cultures, respectively, followed by incubation for 24, 48, 72 or 96 h. Before harvest, 20 μl MTT [3-(4, 5-dimethythiazolzyl)-2, 5-diphenyl tetrazolium tromide, 5 mg/ml; Sigma, St. Louis, MO, USA] was added to each well. After incubating for 4 h, 0.2 ml DMSO was added to stop reactions. The absorbance values of each well were determined spectrophotometrically at 490 nm on Microplate Reader (BIO-TEK, Rockville, MA, USA).

2.3. Fluorescence-activated cell sorting (FACS)

Cell cycle analysis was performed as previously described [24]. Briefly, aliquots of cells (1.5×10^6) were pelleted (1500 rpm, 5 min, 4 °C) and washed twice in ice-cold PBS, and fixed in ice-cold 70% ethanol. Then the cells were washed in PBS and digested with DNase-free RNase A (20 μg/ml) at 37 °C for 30 min. Before FACS analysis, the cells (2×10^4) were resuspended in 200 μl of propidium iodide (10 μg/ml; Sigma) for DNA staining. A FACScan (Becton Dickinson, Franklin Lakes, NJ) was used to analyze cellular DNA content. For cell cycle analysis, computer programs CELLQuest and ModFit LT 2.0ep for power were used. Apoptosis was assayed by the appearance of a sub-G1 (<2N ploidy) population by the computer program CELLQuest.

2.4. Immunocytochemical labeling

Immunocytochemical labeling was performed as previously described [25] with modifications. Briefly, the cells grown on coverslips were fixed with 4% formaldehyde (40% formaldehyde and RPMI 1640, 1:9, pH 6.8) at 37 °C for 30 min, washed in PBS, and then permeabilized with 0.5% Triton X-100 in PBS for 20 min at room temperature. The cells were washed in a blocking solution consisting of 5% BSA and 0.2% Triton X-100 and stored in the blocking solution at 4 °C until labeling. For tubulin labeling, the fixed cells were incubated for 2 h at 37 °C with a primary rat anti-α-tubulin monoclonal antibody (1:100; Chemicon International, Inc., Temecula, CA) in the blocking solution, followed by three washes in the blocking solution. The cells were incubated with a FITC-conjugated goat antirat IgG (1:100) (Sino-American Biotech Co., Beijing, China) in the blocking solution for 1 h at 37 °C and subsequently washed three times, followed by exposure of

cells to rhodamine phalloidin (1:50) (Molecular Probes, Eugene, OR) in the blocking solution for 40 min at 37 °C. Then the cells were incubated for 10 min at room temperature with 5 mg/ml Hoechst 33342 (Molecular Probes). After three washes in PBS, the cells were mounted in a 90% glycerol–PBS mixture. Laser confocal microscopy was performed at room temperature using Leica TCS SP2 (Leica Microsystems Heidelberg GmbH, Mannheim, Germany) confocal microscope equipped with a 63 × /1.4 HCxPlanAPO oil immersion objective. Microtubules were excited with an argon laser (488 nm line), microfilaments with a helium–neon laser (543 nm), and DNA with a UV laser (364 nm). Each image represents a two-dimensional maximum projection of sections in the Z-series taken at 0.5 mm intervals across the depth of the cell.

2.5. *Light scattering assay*

This assay was performed as previously described [26]. Actin (A 3653, Sigma–Aldrich Co) was stored in G-buffer (2 mM Tris [pH 8.0], 0.2 mM $CaCl_2$, 0.2 mM ATP, 0.5 mM DTT). Polymerization was initiated by adding 1 mM $MgCl_2$ in the absence or presence of different concentrations of 8-Cl-ATP and/or ATP. Light scattering was measured at a 90° angle in a cary eclipse fluorescent spectrophotometer (Varian, USA) at 350 nm.

2.6. *DNase I assay for G-actin and total actin*

The assay was performed as previously described [27]. 5×10^6 cells were treated with 300 μl of lysis buffer containing 10 mM K_2HPO_4, 100 mM NaF, 50 mM KCl, 2 mM $MgCl_2$, 1 mM EGTA, 0.2 mM dithiothreitol, 0.5% Triton X-100, 1 M sucrose, pH 7.0. For determination of G-actin content, 10 μl of lysate was added to the assay mixture containing 10 μl of DNase I solution (0.1 mg/ml DNase I in 50 mM Tris–HCl, 10 mM PMSF, 0.5 mM $CaCl_2$, pH 7.5) and 1 ml of DNA solution (40 μg/ml DNA in 100 mM Tris–HCl, 4 mM $MgSO_4$, 1.8 mM $CaCl_2$, pH 7.5). DNase I activity was monitored continuously at 260 nm with a Varian spectrophotometer. Actin in the sample was measured by reference to a standard curve for the inhibition of DNase I activity, prepared with bovine muscle actin (Sigma). A linear relationship was observed over the range of 25–70% inhibition of DNase I activity. To determine total actin, standards or samples were treated on ice for 15 min with an equal volume of guanidine hydrochloride solution to depolymerize F-actin. The depolymerizing solution contained 1.5 M guanidine hydrochloride, 1 M sodium acetate, 1 mM $CaCl_2$, 1 mM ATP, and 20 mM Tris–HCl (pH 7.5). After centrifugation for removing remnant nuclear material, aliquots were combined in a cuvette with DNase I and DNA solutions for actin assay. F-actin was calculated as the difference between total actin and initially measured G-actin. Both G-actin and F-actin contents were related to total protein content. Protein concentrations were measured with BCA protein assay reagent kit (Pierce, Rockford, IL).

2.7. *Western blotting*

Cells for actin measurements were collected on ice and placed in cold lysis buffer (10 mM K_2HPO_4, 100 mM NaF, 50 mM KCl, 2 mM $MgCl_2$, 1 mM EGTA, 0.2 mM dithiothreitol, 0.5% Triton X-100, 1 M sucrose, pH 7.0). The suspension was vortexed or homogenized. The lysate was centrifuged at 15,000 × *g* for 5 min in an Eppendorf microcentrifuge and the supernatant was collected for measurement of soluble actin. For measurement of F-actin, the pellet was resuspended in lysis buffer plus an equal volume of 1.5 M guanidine hydrochloride, 1 M sodium acetate, 1 mM $CaCl_2$, 1 mM ATP, and 20 mM Tris–HCl (pH 7.5). After incubation on ice for 10 min to depolymerize actin filaments, the sample was centrifuged at 15,000 × *g* for 5 min and the supernatant was used for analysis of actin.

Actin content in the Triton X-100 supernatant and pellet was applied on sodium dodecyl sulfate polyacrylamide gel electrophoresis (12% running gel), transferred the protein to nitrocellulose, and probed with specific antibodies for actin (Santa Cruz Biotechnology, Santa Cruz, CA). The blots were developed with a second antibody coupled to horseradish peroxidase. Chemiluminescence signals were visualized using Western blotting luminol reagent (Santa Cruz Biotechnology) and exposed to film.

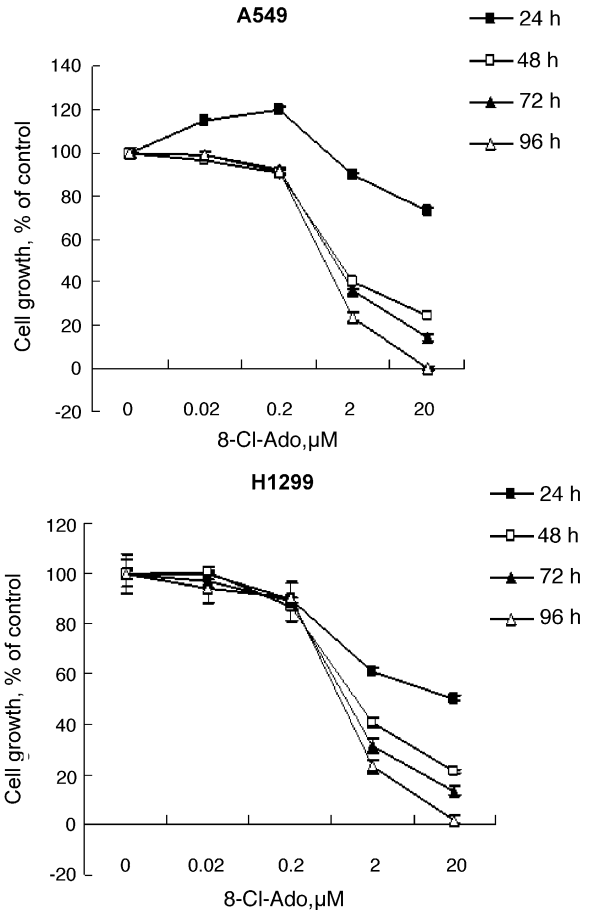

Fig. 1 – Inhibitory effects of 8-Cl-Ado on cell proliferation. Human lung cancer cell lines A549 and H1299 were exposed to 8-Cl-Ado at the indicated concentrations for 24, 48, 72, or 96 h, respectively. Cell proliferation was evaluated with MTT assay. Data represent mean ± S.D. derived from three independent experiments.

2.8. *Invasion and motility assays*

24-Well BD BioCoat™ matrigel invasion chambers were used for invasion and motility assays following the instruction. The lower portion of the invasion chamber was filled with RPMI medium 1640 supplemented with 10% FBS to function as a chemoattractant. For experiments, 2×10^4 cells were placed into each of quadruplicate wells in the upper chamber in serum-free conditions in the presence or absence of 8-Cl-Ado (2 μM). The invasion chamber was incubated at 37 °C under 5% CO_2 in 100% humidity for 48 h as indicated. The polycarbonate filter was then removed, fixed, and stained with HE. Noninvading cells adherent to the upper surface of the filter were wiped off gently with a cotton swab. The percentage of invasion (invading cells attached to under surface of the filter) was determined for each well by calculating the percentage of the well filter surface area occupied by invading cells.

2.9. *Statistical analysis*

The Student's *t*-test and ANOVA test were used for univariate analysis. Statistical significance was defined by a two-tailed *P*-value of 0.05.

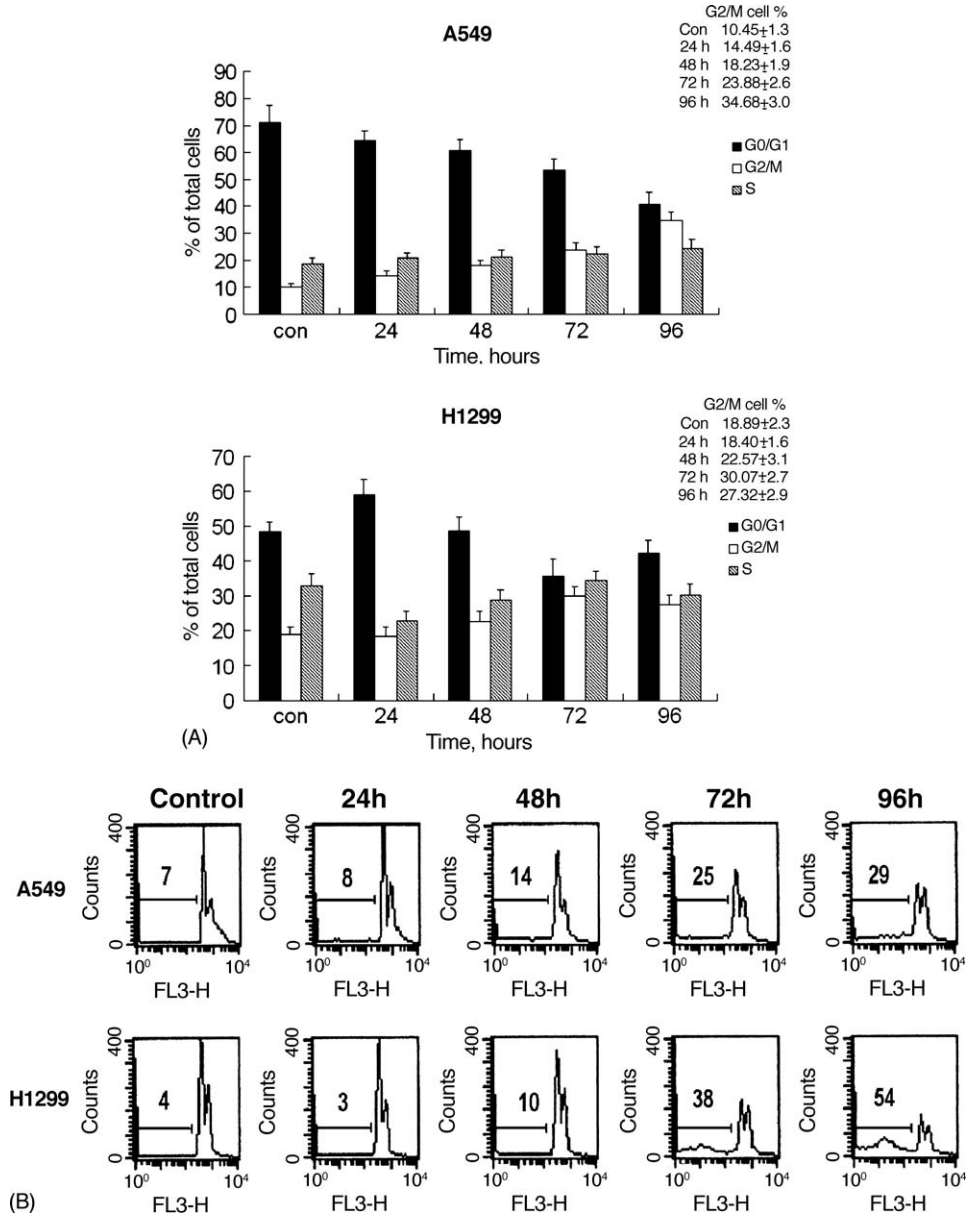

Fig. 2 – 8-Cl-Ado-induced G2/M arrest and apoptosis in cultured cancer cells. (A) Histograms showing the populations of the cell cycle. A549 and H1299 cells were unexposed or exposed to 8-Cl-Ado (2 μg) for 24, 48, 72 and 96 h, respectively. The cells (2×10^4) were fixed with 70% ethanol and stained with propidium iodide (PI); PI signal was measured by FACScan. G1, G2/M and S populations in the cell cycle were analyzed by computer programs (see text). Data represent mean ± S.D. derived from three independent experiments. (B) Analysis of apoptosis. Cell exposure and staining are the same as in (A). Apoptotic cells with a sub-G1 (<2N ploidy) were assayed by the computer program CELLQuest. Data represent one of three independent experiments. *Note*: marked apoptosis occurred after 48–72 h exposure.

3. Results

3.1. 8-Cl-Ado-induced inhibitory proliferation of A549 and H1299 cells

With MTT method we analyzed the inhibitory effects of 8-Cl-Ado on A549 and H1299 cells. The time- and dose-effect curves revealed that 8-Cl-Ado (≥2 μM) caused significant growth inhibition of A549 and H1299 cells within 24–96 h after exposure (Fig. 1). To determine whether the inhibition of cell growth by 8-Cl-Ado is closely related to cell-cycle control or apoptosis, we analyzed the cell-cycle distribution of the tumor cells with fluorescence activated cell sorter (FACS). As we have previously reported [24], exposure of A549 cells to 2 μM 8-Cl-Ado caused the increases from 14.49% to 34.68% of G2/M subpopulation within 24–96 h, compared with unexposed cells that showed 10.15% G2/M subpopulation. In H1299 cells, 8-Cl-Ado-induced accumulation of G2/M phase was from 18.4% to 27.32%, compared with 18.89% G2/M in unexposed cells. Both A549 and H1299 cells exposed to 8-Cl-Ado showed a time-dependent increase in G2/M subpopulation within 24–96 h (Fig. 2A). However, no obvious sub-G1 cells (apoptotic cells) were observed before 48 h exposure. The A549 and H1299 cells increased sub-G1 DNA content characterizing apoptosis within 48–96 h of exposure (Fig. 2B). Our results indicate that 8-Cl-Ado induces inhibitory proliferation is mainly due to accumulation of cells in G2/M phase followed by apoptosis.

3.2. Alteration of actin organization and morphology in targeted cells

Because microfilaments as well as microtubules are essential for cell division, and their disruption can induce G2/M arrest and apoptosis [25], triple fluorescence labeling was employed to analyze cell morphology. Cytoskeleton immunocytochemistry revealed that actin displayed filament bundles or stress fibers surrounding the unexposed cells, showing a similar indication of cell morphology. As early as 24–48 h after

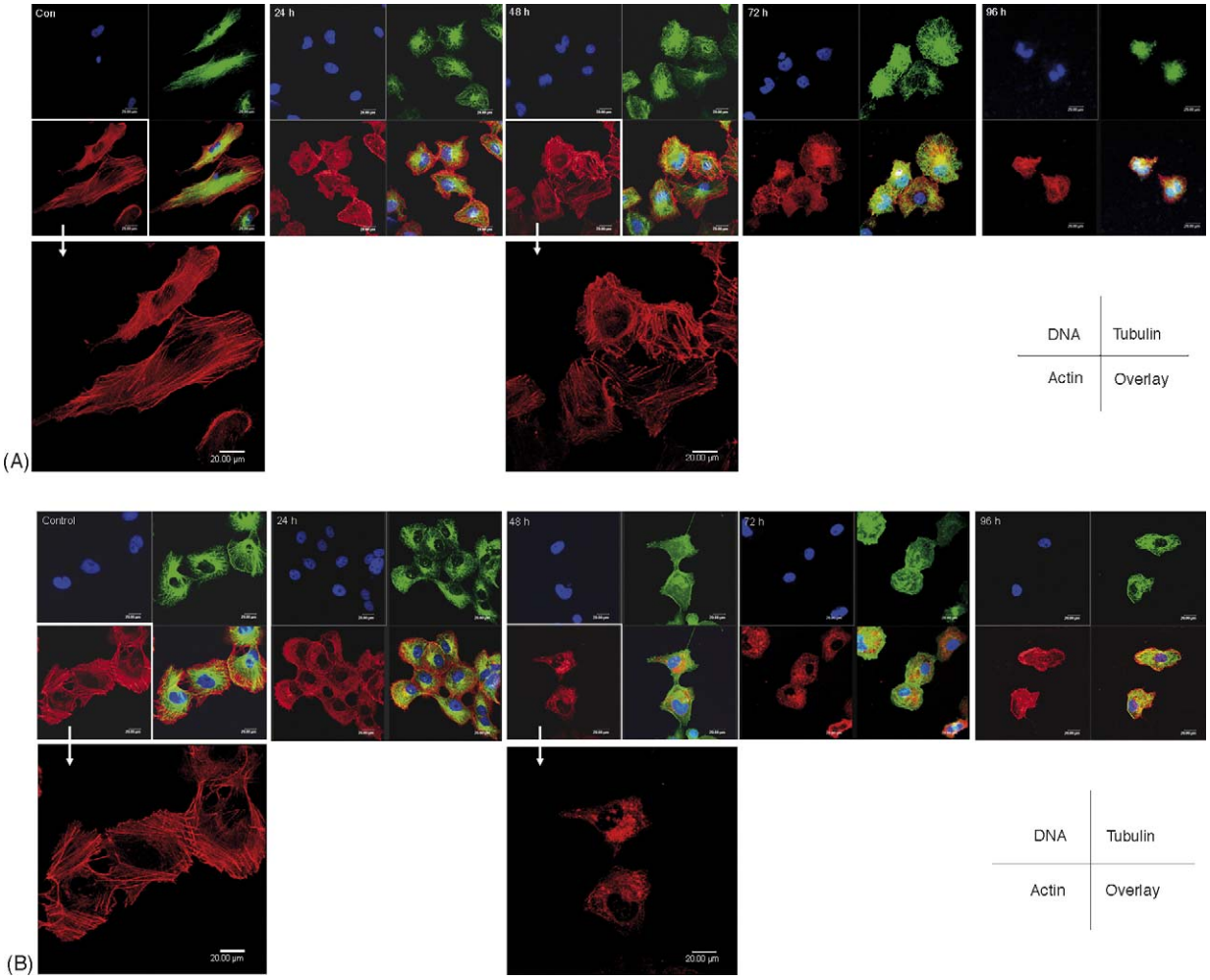

Fig. 3 – Cytoskeletal disruption and morphological change (in size and shape) induced by 8-Cl-Ado. A549 (A) and H1299 (B) cells were exposed as described in Fig. 2. After cell fixation and permeabilization, the nuclei were stained with Hoechst 33342 (blue), actin filaments were stained with rhodamine-phalloidin (red), microtubules were labeled with a primary rat anti-α-tubulin monoclonal antibody and FITC-conjugated goat antirat IgG (green). The cells were examined with a Leica TCS-SP2 confocal microscope. Microtubules were excited with an argon laser (488 nm line), microfilaments with a helium–neon laser (543 nm), and DNA with a UV laser (364 nm). Scale bar, 20 μm.

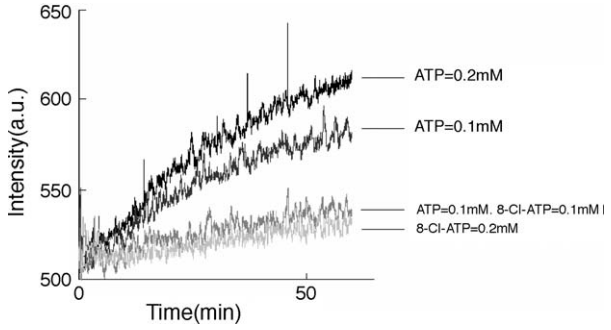

Fig. 4 – Time course for actin polymerization in the presence of 8-Cl-ATP. Monomeric G-actin (2 mM) was stored in G-buffer (see Section 2). Polymerization was initiated by adding 1 mM $MgCl_2$ in the absence or presence of different concentrations of 8-Cl-ATP and/or ATP. Actin polymerization was monitored as an increase in light scattering, and measured at a 90° angle in a cary eclipse fluorescent spectrophotometer at 350 nm.

8-Cl-Ado exposure, there was no obvious death in A549 and H1299 cells. Whereas, the cells differed in size and shape and the cell mass became smaller and the cell body was shrunken after 24 h exposure. Some of the exposed cells were binucleated, multinucleated or micronucleus, indicating dividing failure and mitotic catastrophe. Notably, the cells had the altered fibrillar array of actin filaments that were greatly abrupt and characterized by the presence of short and stress fibers in the cytoplasm (Fig. 3). Along with the time of exposure to 8-Cl-Ado, actin skeleton was disrupted more apparently. By 72–96 h, the skeleton network was almost collapsed. In the same experiments, we also found that the microtubule organization was changed in exposed cells.

3.3. *Inhibition of in vitro polymerization of G-actin to F-actin by 8-Cl-ATP*

Because the interconversion between ATP and ADP forms of actin is important in the assembly of actin cytoskeleton [2], and the conversion of 8-Cl-Ado to 8-Cl-ATP may exhaust ATP pool in the cells [17], we speculate that 8-Cl-ATP can interfere with the actin dynamics. Light scattering assays of actin *in vitro* were performed (Fig. 4) and showed that 0.2 mM 8-Cl-ATP could markedly inhibit the polymerization of monomeric actin in 60 min recorded and 0.1 mM 8-Cl-ATP with 0.1 mM ATP gave similar inhibitory effect. However, adding 0.1 mM or 0.2 mM ATP to a solution of G-actin induced the polymerization of G-actin into F-actin filaments. These evidences indicate that both decrease of ATP and increase of 8-Cl-ATP are responsible for inhibiting the polymerization of monomeric actin.

3.4. *Increase in G-actin/F-actin ratio in 8-Cl-Ado-exposed cells*

Because 8-Cl-ATP can inhibit the polymerization of G-actin into F-actin *in vitro*, and 8-Cl-ATP is the metabolite of 8-Cl-Ado in living cells, it is fully reasonable to infer that actin polymerization status in 8-Cl-Ado-exposed cells differs from the control cells. To test this idea DNase I inhibition assay was employed for measuring quantitative changes in actin polymerization dynamics in living cells. As expected, after 48 h exposure to 8-Cl-Ado, the G/F-actin ratio, as a surrogate marker of actin polymerization status in cells, in exposed A549 cells was 1.57, which was significantly higher than the G/F-actin ratio of 1.08 in unexposed A549 cells. Similarly, the G/F ratio in exposed H1299 cells was 1.83, compared to 1.31 in unexposed H1299 cells (Table 1 and Fig. 5). The results were in accordance with the observation in light scattering assays. In the DNase I inhibition experiments, however, cytochalasin B (CB), a drug known to induce microfilament depolymerization, had no significant effect on the ratio of G- to F-actin in CB-exposed cells. These data suggest that the mechanism of 8-Cl-Ado act differs from that of CB that does not produce net depolymerization of the actin filaments [28,29].

3.5. *Increase in actin content in soluble cell extracts after 8-Cl-Ado exposure*

Since 8-Cl-Ado exposure induced G/F ratio increase in A549 and H1299 cells, we determined the actin contents in soluble and insoluble cell extracts by use of anti-actin antibodies. Western blotting showed that the actin content in insoluble cell extracts was markedly decreased after 8-Cl-Ado exposure, and the proportion of soluble actin to insoluble actin in exposed cells was much higher than that in unexposed cells (control), which was similar to that in the same experiments with CB (Fig. 6). Our data indicate that both 8-Cl-Ado and CB can interfere with the dynamic instability of microfilaments, but their mechanisms are different from each other (see Section 4).

Table 1 – The effects of 8-Cl-Ado on actin polymerization in living cells

Treatment	G/F-actin ratio	G-actin/protein (μg/mg)	F-actin/protein (μg/mg)	Total actin/protein (μg/mg)
A549 control	1.08 ± 0.27	27.4 ± 4.6	26.3 ± 4.7	53.7 ± 4.1
A549-8-Cl-Ado	1.57 ± 0.35	34.5 ± 3.8	22.4 ± 2.7	56.9 ± 3.7
H1299 control	1.31 ± 0.17	25.2 ± 2.9	20.4 ± 1.5	45.6 ± 3.9
H1299-8-Cl-Ado	1.83 ± 0.27	28.4 ± 2.2	16.6 ± 3.3	43.8 ± 4.8

For determining total actin, samples were treated with an equal volume of guanidine hydrochloride solution to depolymerize F-actin. G-actin in the sample was measured by reference to a standard curve for the inhibition of DNase I activity. F-actin was calculated as the difference between total actin and initially measured G-actin. Both G-actin and F-actin contents were related to total protein content measured with BCA protein assay reagent kit. Data present mean ± S.D. from three independent experiments. $^{*}P < 0.05$.

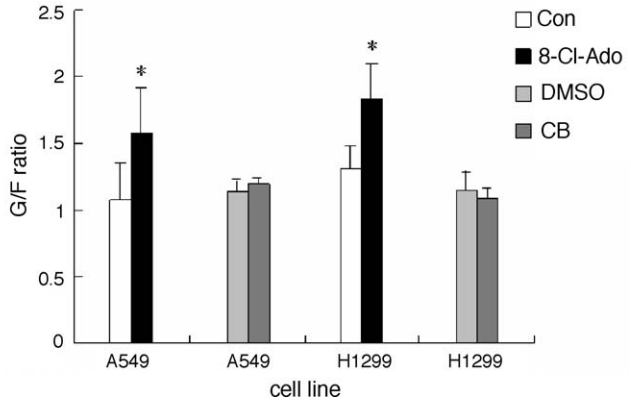

Fig. 5 – DNase I inhibition assays of G-actin/F-actin ratio in living A549 and H1299 cells. A549 and H1299 cells were incubated with 2 μM 8-Cl-Ado for 0 (control) or 48 h and 2 μg/ml Cytochalasin B (CB) for 0 (DMSO) or 48 h, respectively. The ratio of total G-actin to F-actin was determined by DNase I inhibition assays. Data present mean ± S.D. from three independent experiments performed with duplicates. The asterisk denotes statistical significance at a level of confidence $P < 0.05$ vs. control.

3.6. *Effect of 8-Cl-Ado exposure on cell motility*

We have showed that actin cytoskeleton disruption induced by 8-Cl-Ado arrested cells in G2/M phase (Fig. 2) and prevented cell division [24]. In order to further demonstrate the functional signification of altered actin organization during 8-Cl-Ado exposure, cell migration and invasion as ability of cell motility were examined by an *in vitro* study of cell invasion through basement membrane. Fig. 7A showed the micrographs of a typical transwell experiment where transmigrated cells were seen. A minimum of 100 transmigrated cells from three independent experiments was counted for examining inhibition of cell migration. As shown in Fig. 7B, 8-Cl-Ado led to the invision decreased to 35.16% and 8.64% in exposed A549 and H1299 cells, when compared to 68.71% and 39.35% in unexposed cells, respectively. These results suggest that 8-Cl-Ado exposure did weaken cell attachment and adhesion, thereby decreasing cell motility and invasion, which may result from actin cytoskeleton disruption.

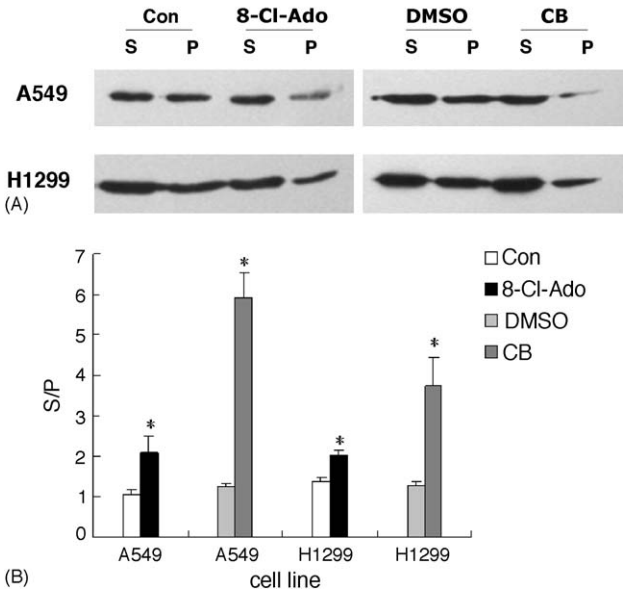

Fig. 6 – Western blotting analyses of soluble- and insoluble-actin. A549 and H1299 cells were exposed to 8-Cl-Ado or CB as described in Fig. 5. The cells were extracted with Triton X-100 buffer. (A) G- actin and F-actin in supernatant (S) and pellet (P) fractions were analyzed by Western blotting. The data represent one of three independent experiments. (B) The relative actin levels in each treatment were expressed as S/P. Data represent mean ± S.D. derived from three independent experiments.

4. Discussion

We demonstrate that 8-Cl-Ado exposure can interfere with the dynamic state of actin polymerization, perturbing the formation of actin stress fiber and decreasing the size of cells. 8-Cl-Ado-induced disorder of network of actin skeleton is responsible at least in part to its inhibitory effects on cell proliferation and cell death including apoptosis and mitotic catastrophe in A549 and H1299 cells.

Recent studies demonstrate that 8-Cl-cAMP exerts its cytotoxicity by converting into its metabolite, 8-chloroadenosine (8-Cl-Ado) [9,17,18,20,21]. In living cells 8-Cl-Ado can be phosphorylated to the moiety of 8-Cl-ATP that inhibits the tumor cell proliferation through inhibition of RNA synthesis [17,18,22,23]. However, no research dealt with the effect of 8-Cl-ATP on actin filaments. A key feature of actin is its ability to bind and hydrolyze ATP. The transition from ATP-bound actin to ADP-bound actin is accompanied by a conformational change that is crucial to the dynamic turnover of actin filaments. Therefore we tested the hypothesis that 8-Cl-Ado can interfere with the dynamics of actin assembly. In most cells approximately 50% of the total actin is present in the form of F-actin and the other 50% is present as G-actin [27]. We found that the G-actin/F-actin ratios in unexposed (control) A549 and H1299 cells were 1.08 and 1.31, respectively. However, G-actin/F-actin ratio in 8-Cl-Ado-exposed A549 cells was 1.60, and that in exposed H1299 cells was 1.83, respectively (Fig. 5). We thus speculate that 8-Cl-Ado can inhibit the polymerization of monomeric actin in living cells through converting to 8-Cl-ATP. This idea was evidenced by *in vitro* light scattering assay of actin, which showed that 8-Cl-ATP directly inhibited the ability of G-actin polymerizing into F-actin (Fig. 4). In addition, we found that the actin cytoskeleton was disorganized in all bundles and networks in targeted cells after 24 h exposure (Fig. 3), suggesting that 8-Cl-Ado may affect the kinetics of both polymerization of G-actin and depolymerization of F-actin, which is important for maintaining normal structure of actin filaments.

The disruption of the integrity of actin cytoskeleton prevents nuclear division, which is controlled by the activation of morphogenesis checkpoint [3]. It is demonstrated that the cells with a completely depolymerized actin cytoskeleton arrest in G2/M phase, due to an inability to reach the mitotic size threshold, suggesting that G2/M arrest caused by actin

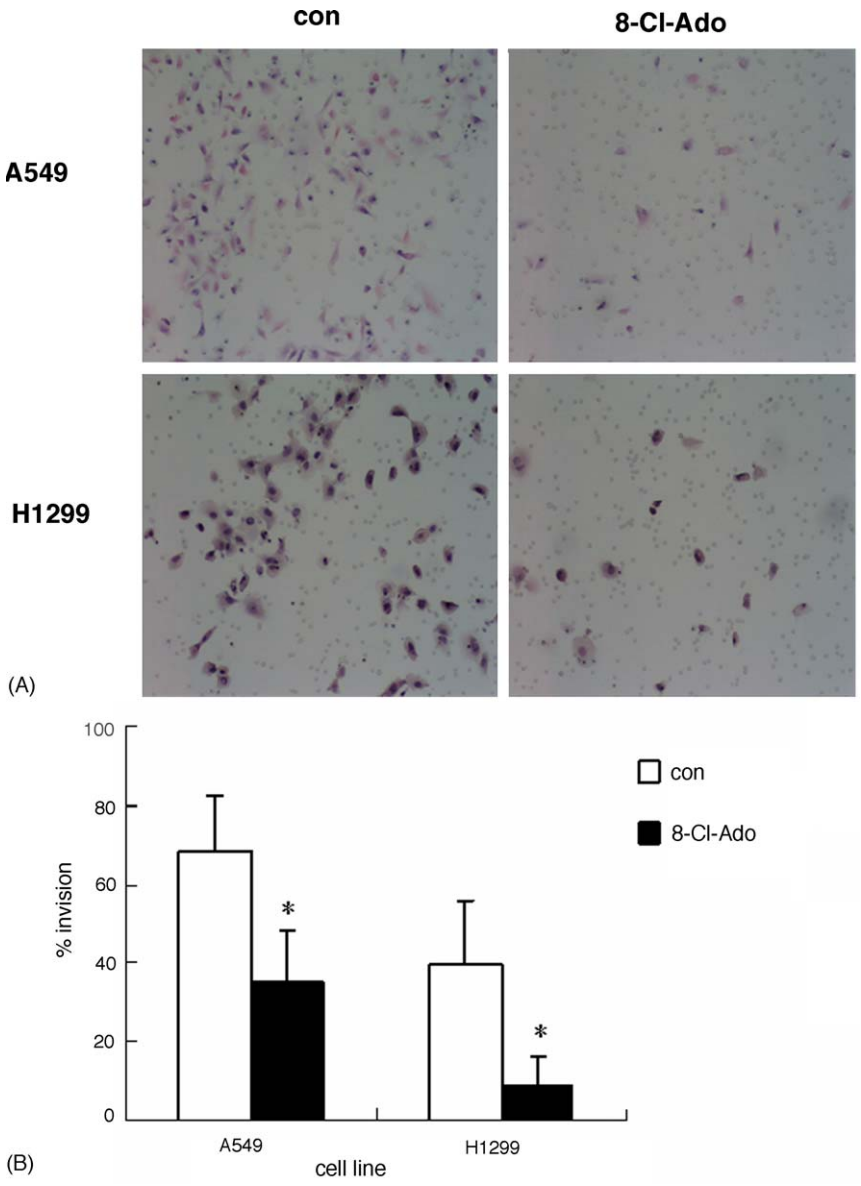

Fig. 7 – Effect of 8-Cl-Adenosine on cell motility. 24-well BD BioCoat™ matrigel invasion chambers were used for invasion and motility assays following the instruction. A549 and H1299 cells (2×10^4) were placed into each of quadruplicate wells in the upper chamber in serum-free conditions in the presence or absence of 8-Cl-Ado (2 μM), incubated at 37 °C under 5% CO_2 in 100% humidity for 48 h. (A) Micrographs of transwells showing transmigrated cells that have been stained with HE. Magnification 100×; (B) Histograms showing inhibitory cell migration. Data is expressed as the percent invasion through the matrigel matrix and membrane relative to the migration through the control membrane. A minimum of 100 transmigrated cells from three independent experiments was counted. Values represent mean ± S.D. $^*P < 0.05$.

disruption is a manifestation of the cell size checkpoint [4]. In this study we found that 8-Cl-Ado exposure could inhibit the polymerization of actin. Actin depolymerization greatly perturbed the filament organization in 8-Cl-Ado-exposed-cells, resulting in the reduction of the size of targeted cells and the accumulation of G2/M population and the aberrant mitosis (Figs. 2 and 3). We have previously reported that the G2/M arrest in 8-Cl-Ado-exposed cells involves the inhibitory phosphorylation of Cdc2-Tyr15 and Cdc25C-Ser216 [24]. The Cdc2-Tyr15 dephosphorylation pathway is targeted by the cell size-monitoring system, where the Cdc25 protein tyrosine phosphatase is required to link cell size monitoring to mitotic control [3,4]. Thus, we suggest that 8-Cl-Ado has activity as an inhibitor of actin polymerization, which may activate the signaling pathway of the morphogenesis checkpoint or the cell size checkpoint.

We have described that 8-Cl-Ado can inhibit cancer cell growth by induction of G2/M arrest and chromosome segregation failure [24]. In those studies, however, we have not clarified the mechanism of 8-Cl-Ado act on actin organization. In the present study we demonstrated that 8-Cl-Ado exposure could affect the dynamic instability of actin,

perturbing the functions of the actin cytoskeleton. Probably, there are three ways by which 8-Cl-Ado may directly or indirectly interfere with actin polymerization in target cells. First, exposure to 8-Cl-Ado accumulates monophosphates and triphosphates of 8-Cl-adenosine in living cells [17,18]. Therefore, the elimination of cellular ATP pool may block ATP-dependent polymerization of G-actin into F-actin filaments. Second, 8-Cl-ATP, as an ATP analogue, may competitively bind to the ATP binding site on G-actin, inhibiting the polymerization of G-actin into F-actin. This notion is supported by light scattering assay and DNase I inhibition assay (Figs. 4 and 5). Third, both polymerization and depolymerization of actin filaments depend on the dynamic instability of actin, whose regulation involves actin binding proteins and complex signal transduction [2,30,31]. For example, the activation of the Rho/Rac/Cdc42 family is linked to the regulation of actin depolymerization through PAK1 (p21-associated kinase 1) and LIM kinase. 8-Cl-ATP may interfere with some signal pathways that affect the function of actin cytoskeleton, which needs to be studied.

Since cytochalasins have long been used as probes for studying actin-based motility and cytoskeletal structure [32,33], we compared the effects of 8-Cl-Ado with cytochalasin B (CB) on actin polymerization in A549 and H1299 cells. 8-Cl-Ado could change the G-/F-actin ratios in both DNase I inhibition assay and Western blotting. In contrast with 8-Cl-Ado, the G-/F-actin ratio in DNase I inhibition assays was not changed, but the insoluble actin significantly decreased in Western blotting after CB exposure (Fig. 5). CB-induced inconsistent G-/F-actin ratios in both experiments may be due to the character of DNase I inhibition assay that determines the G-actin and the F-actin was calculated as the difference between total actin and measured G-actin. Alternatively, this method does not distinguish the dimmer/oligomer of actin from long actin filament (F-actin) [29]. Another explanation is the different mechanism. It has been reported that CB does not affect the G/F-actin ratio in living cells [34]. Similarly, neither short- nor long-term exposure of living HEp-2 cells to cytochalasin D (CD) produce net depolymerization of filamentous actin [29]. It has been postulated that the cytochalasins slow the rate of filament polymerization by inhibiting elongation, but do not prevent monomer addition onto the barbed ends of the acrosomal actin filaments [28,29,32–34]. In our case, however, 8-Cl-Ado may inhibit both initial nucleation and elongation of actin assembly. Further understanding of the mechanisms of 8-Cl-Ado act is required.

It should be noted that both actin and microtubule cytoskeletal systems play key roles in cellular processes including generation and maintenance of cell morphology and polarity, in endocytosis and intracellular trafficking, and in contractility, motility and cell division [1]. In this study we have only discussed the alteration of actin cytoskeleton during 8-Cl-Ado exposure. In fact, the microtubule cytoskeletal system was also changed in 8-Cl-Ado-exposed cells (Fig. 3). It has recently been reviewed that there are the physical connections and the potential functional links between two cytoskeletal systems. The physical connections imply the existence of bifunctional linking proteins or a series of protein–protein interactions (for example Kar9p); the functional links mean that the function of one cytoskeletal system indirectly affects some aspect of the other system [35,36]. Since the depletion of cellular ATP pool by 8-Cl-Ado can block the transfer of γ-phosphate from ATP to GDP for generating GTP and the hydrolysis of GTP bound to tubulin is the heart of the rapid turnover of microtubules, the reorganization of microtubule may be inhibited. Here we did find the inhibition of tubulin polymerization. The exact mechanism for tubulin disruption is presently unknown.

Some studies demonstrate that 8-Cl-adenosine derivates induce apoptosis in tumor cells [9,13,14,16,17,19]; others suggest that 8-Cl-adenosine derivates induce differentiation of targeted cells [8,12,19]. We have previously showed that mitotic catastrophe is a major event in 8-Cl-Ado-exposed human lung cancer cells [24]. Decisions whether to die by apoptotic or non-apoptotic cell death involve specific lesion and module as well as cell type. The regulations of protein kinase A [12], protein kinase C [37] and p38 MAP kinase [38] in the inhibitory proliferation of 8-Cl-cAMP- and 8-Cl-Ado-targeted cells have been reported. The heart of the mechanisms of 8-Cl-Ado act is that 8-Cl-Ado exerts its cytotoxicity by converting into 8-Cl-ATP [17,18]. 8-Cl-Ado may induce inhibitory proliferation of exposed cells by targeting cellular bioenergy and RNA transcription and translation [17,18,20–22]. 8-Cl-ATP can also interfere with all biochemical reactions that need ATP. These facts indicate that 8-Cl-Ado actions are at multiple levels and its mechanisms are complicated. Therefore, 8-Cl-Ado act on actin organization may at least partly afford this effect, which does not exclude other possibilities.

Acknowledgements

This work was funded by National Natural Science Foundation of PR China grants 30271448, 30471975, 30393113 and Education Ministry of P. R. China grant 03003. We thank Lan Yuan for assistance with confocal analysis.

REFERENCES

[1] Lodish H, Berk A, Zipursky SL, Matsudaira P, Baltimore D, Darnell J. Mol Cell Biol. 4th ed New York: Scientific American Books; 2000.
[2] Jordan MA, Wilson L. Microtubules and actin filaments: dynamic targets for cancer chemotherapy. Curr Opin Cell Biol 1998;10:123–30.
[3] Lew DJ. Cell-cycle checkpoints that ensure coordination between nuclear, and cytoplasmic events in *Saccharomyces cerevisiae*. Curr Opin Genet Dev 2000;10:47–53.
[4] Rupe I, Webb BA, Mak A, Young PG. G2/M arrest caused by actin disruption is a manifestation of the cell size checkpoint in fission yeast. Mol Biol Cell 2001;12:3892–903.
[5] Gordon SR, Climie M, Hitt AL. 5-Fluorouracil interferes with actin organization, stress fiber formation and cell migration in corneal endothelial cells during wound repair along the natural basement membrane. Cell Motil Cytoskeleton 2005;62:244–58.
[6] Lu QY, Jin YS, Zhang Q, Zhang Z, Heber D, Go VL, et al. Ganoderma lucidum extracts inhibit growth and induce actin polymerization in bladder cancer cells in vitro. Cancer Lett 2004;216:9–20.

[7] Bing W, Razzaq A, Sparrow J, Marston S. Tropomyosin and troponin regulation of wild type and E93K mutant actin filaments from *Drosophila* flight muscle. J Biol Chem 1998;273:15016–21.
[8] Tortora G, Pepe S, Yokozaki H, Meissner S, Cho-Chung YS. Cooperative effect of 8-Cl-cAMP and rhGM-CSF on the differentiation of HL-60 human leukemia cells. Biochem Biophys Res Commun 1991;177:1133–40.
[9] Halgren RG, Traynor AE, Pillay S, Zell JL, Heller KF, Krett NL, et al. 8Cl-cAMP cytotoxicity in both steroid sensitive and insensitive multiple myeloma cell lines is mediated by 8Cl-Adenosine. Blood 1998;92:2893–8.
[10] Langeveld CH, Jongenelen CA, Heimans JJ, Stoof JC. Growth inhibition of human glioma cells induced by 8-chloroadenosine, an active metabolite of 8-chloro cyclic adenosine 3′:5′-monophosphate. Cancer Res 1992;52:3994–9.
[11] Ally S, Clair T, Katsaros D, Tortora G, Yokozaki H, Finch RA, et al. Inhibition of growth and modulation of gene expression in human lung carcinoma in athymic mice by site-selective 8-Cl-cyclic adenosine monophosphate. Cancer Res 1989;49:5650–5.
[12] Rohlff C, Clair T, Cho-Chung YS. 8-Cl-cAMP induces truncation and down-regulation of the RI alpha subunit and up-regulation of the RII beta subunit of cAMP-dependent protein kinase leading to type II holoenzyme-dependent growth inhibition and differentiation of HL-60 leukemia cells. J Biol Chem 1993;268:5774–82.
[13] Kim SN, Ahn YH, Kim SG, Park SD, Cho-Chung YS, Hong SH. 8-Cl-cAMP induces cell cycle-specific apoptosis in human cancer cells. Int J Cancer 2001;93:33–41.
[14] Grbovic O, Jovic V, Ruzdijic S, Pejanovic V, Rakic L, Kanazir S. 8-Cl-cAMP affects glioma cell-cycle kinetics and selectively induces apoptosis. Cancer Invest 2002;20:972–82.
[15] Taylor CW, Yeoman LC. Inhibition of colon tumor cell growth by 8-chloro-cAMP is dependent upon its conversion to 8-chloro-adenosine. Anticancer Drugs 1992;3:485–91.
[16] Carlson CC, Chinery R, Burnham LL, Dransfield DT. 8-Cl-adenosine-induced inhibition of colorectal cancer growth in vitro and in vivo. Neoplasia 2000;2:441–8.
[17] Gandhi V, Ayres M, Halgren RG, Krett NL, Newman RA, Rosen ST. 8-Chloro-cAMP and 8-Chloro-adenosine act by the same mechanism in multiple myeloma cells. Cancer Res 2001;61:5474–9.
[18] Stellrecht CM, Rodriguez Jr CO, Ayres M, Gandhi V. RNA-directed actions of 8-Chloro-adenosine in multiple myeloma cells. Cancer Res 2003;63:7968–74.
[19] Fassina G, Aluigi MG, Gentleman S, Wong P, Cai T, Albini A, et al. The cAMP analog 8-Cl-cAMP inhibits growth and induces differentiation and apoptosis in retinoblastoma cells. Int J Cancer 1997;72:1088–94.
[20] Lange-Carter CA, Vuillequez JJ, Malkinson AM. 8-Chloroadenosine mediates 8-chloro-cyclic AMP-induced down-regulation of cyclic AMP-dependent protein kinase in normal and neoplastic mouse lung epithelial cells by a cyclic AMP-independent mechanism. Cancer Res 1993;53:393–400.
[21] Robbins SK, Houlbrook S, Priddle JD, Harris AL. 8-Cl-adenosine is an active metabolite of 8-Cl-cAMP responsible for its in vitro antiproliferative effects on CHO mutants hypersensitive to cytostatic drugs. Cancer Chemother Pharmacol 2001;48:451–8.
[22] Chen LS, Sheppard TL. Synthesis and hybridization properties of RNA containing 8-chloroadenosine. Nucleosides Nucleotides Nucleic Acids 2002;21:599–617.
[23] Chen LS, Sheppard TL. Chain termination and inhibition of *Saccharomyces cerevisiae* poly(A) polymerase by C-8-modified ATP analogs. J Biol Chem 2004;279:40405–11.
[24] Zhang H-Y, Gu Y-Y, Li Z-G, Jia Y-H, Yuan L, Li S-Y, et al. Exposure of human lung cancer cells to 8-chloro-adenosine induces G2/M arrest and mitotic catastrophe. Neoplasia 2004;6:802–12.
[25] Yamazaki Y, Tsuruga M, Zhou D, Fujita Y, Shang X, Dang Y, et al. Cytoskeletal disruption accelerates caspase-3 activation and alters the intracellular membrane reorganization in DNA damage-induced apoptosis. Exp Cell Res 2000;259:64–78.
[26] Blader IJ, Cope MJV, Jackson TR, Profit AA, Greenwood AF, Drubin DG, et al. GCS1, an Arf guanosine triphosphatase-activating protein in *Saccharomyces cerevisiae*, is required for normal actin cytoskeletal organization in vivo and stimulates actin polymerization in vitro. Mol Biol Cell 1999;10:581–96.
[27] Heacock CS, Bamburg JR. The quantitation of G- and F-actin in cultured cells. Anal Biochem 1983;135:22–36.
[28] Bonder EM, Mooseker MS. Cytochalasin B slows but does not prevent monomer addition at the barbed end of the actin filament. J Cell Biol 1986;102:282–8.
[29] Morris A, Tannenbaum J. Cytochalasin D does not produce net depolymerization of actin filaments in HEp-2 cells. Nature 1980;287:637–9.
[30] Feldner JC, Brandt BH. Cancer cell motility—on the road from c-erbB-2 receptor steered signaling to actin reorganization. Exp Cell Res 2002;272:93–108.
[31] Edwards DC, Sanders LC, Bockoch GM, Gill GN. Activation of LIM-kinase by Pak1 couples Rac/Cdc42 GTPase signaling to actin cytoskeletal dynamics. Nat Cell Biol 1999;1:253–9.
[32] Weihing RR. Cytochalasin B inhibits actin-related gelatin of Hela cell extracts. J Cell Biol 1976;71:303–7.
[33] Wessells NK, Spooner BS, Ash JF, Bradley MO, Luduena MA, Taylor EL, et al. Microfilaments in cellular and developmental processes. Science 1971;171:135–43.
[34] Baatout S, Chatelain B, Staquet P, Symann M, Chatelain C. Induction and enhancement of normal human megakaryocyte polyploidization are concomitant with perturbation in the actin metabolism. Eur J Clin Invest 1998;28:845–55.
[35] Goode BL, Drubin DG, Barnes G. Functional cooperation between the microtubule and actin cytoskeletons. Curr Opin Cell Biol 2000;12:63–71.
[36] Yarm F, Sagot I, Pellman D. The social life of actin and microtubules: interaction versus cooperation. Curr Opin Microbiol 2001;4:696–702.
[37] Ahn YH, Jung JM, Hong SH. 8-Cl-cAMP and its metabolite, 8-Cl-adenosine induce growth inhibition in mouse fibroblast DT cells through the same pathways; protein kinase C activation and cyclin B downregulation. J Cell Physiol 2004;201:277–85.
[38] Ahn YH, Jung JM, Hong SH. 8-Chloro-cyclic AMP-induced growth inhibition and apoptosis is mediated by p38 mitogen-activated protein kinase activation in HL60 cells. Cancer Res 2005;65:4896–5901.